Spectroscopic, Calorimetric, and Kinetic Demonstration of Conformational Adaptation in Peptide−Antibody Recognition†

Lukas Leder, Christine Berger, Susanne Bornhauser, Hans Wendt,‡ Friederike Ackermann, Ilian Jelesarov, and Hans Rudolf Bosshard*

Biochemisches Institut der Universität Zürich, Winterthurerstrasse 190, CH-8057 Zürich, Switzerland

Received July 10, 1995; Revised Manuscript Received September 25, 1995⊗

ABSTRACT: Little is known about the extent to which protein flexibility contributes to antigen−antibody recognition and cross-reactivity. Using short coiled coil peptides (leucine zippers) as model antigens, we demonstrate that a monoclonal antibody can force a noncognate peptide into a conformation that is similar to the conformation of the cognate peptide against which the monoclonal antibody is directed. Monoclonal antibodies 29AB and 13AD were raised against the 29-residue peptide LZ (Ac-EYEALEKKLAALE-AKLQALEKKLEALEHG-amide) that forms a very stable coiled coil. The two antibodies cross-reacted strongly with the random coil analogue LZ(7P14P) that contains Lys→Pro and Ala→Pro substitutions in positions 7 and 14, respectively. The antibody-bound peptide LZ(7P14P) adopted an altered conformation that possibly was coiled coil-like, as shown by CD difference spectroscopy and fluorescence quenching experiments on coumarin-labeled peptides. Isothermal titration calorimetry revealed that the cross-reaction of antibodies 13AD and 29AB with the random coil peptide LZ(7P14P) exhibited a large unfavorable entropy. This, however, was strongly compensated by a more favorable enthalpy, resulting in only a small difference between the association constants for peptide LZ and LZ(7P14P), respectively. To investigate the opposite type of cross-reaction, monoclonal antibody 42PF was raised against the random coil peptide LZ(7P14P). 42PF cross-reacted with coiled coil peptide LZ by forcing it to dissociate into single chains. Enthalpy/entropy compensation again enabled the cross-reaction, which now was entropically favored and enthalpically disfavored. The rate of reaction of antibody 42PF with peptide LZ was controlled by the rate of dissociation of LZ into single chains. This observation, as well as the generally much slower reaction rate with the noncognate peptides, indicated that the cross-reactivity occurred because the antibody selected the conformer of the antigen that binds the strongest, a mechanism we call "induced fit by conformational selection".

There is much interest in deciphering the molecular basis of the antigenic cross-reactivity of antibodies. The topic bears strongly on the application of peptides to produce antibodies that react with intact proteins, one of the prerequisites for the success of peptide vaccines (Arnon & Van Regenmortel, 1992). Reciprocal conformational adaptation of the antigen and the antibody bringing the contacting residues of antigen and antibody closer to each other is seen in the crystal structures of some protein−antibody complexes. Changes in the antibody may involve subtle adjustments of side chain dihedral angles and backbone conformations (Tulip et al., 1992; Roberts et al., 1987), rearrangements of loops (Rini et al., 1992), and small reciprocal movements of V_H and V_L domains (Bhat et al., 1990, 1994). Adjustments in the antigen are also variable, and some significant rearrangements have been observed with peptides (Stanfield et al., 1990; Stanfield & Wilson, 1993; Wilson & Stanfield, 1994; Wien et al., 1995) and oligosaccharides (Bundle et al., 1994). On the whole, however, extensive changes of the antigen and antibody structure are rare, and many complexes resemble the lock-and-key paragon. Nevertheless, the recurrent observation of antibodies cross-reacting with dissimilar, though mostly related, antigens would seem to indicate that conformational adaptation has to play a role in antibody recognition. In particular, the reaction of a protein-reactive antibody with a peptide, or of a peptide-reactive antibody with the corresponding sequence of the intact protein, may follow an induced fit mechanism to which both the antigen and the antibody can contribute. The major unanswered questions are, (i) Does antibody cross-reactivity relax the requirement for a preexisting precise fit between free antigen and free antibody? (ii) How can antigen−antibody complementarity be preserved through reciprocal conformational adaptation of the molecules?

Here we demonstrate that very substantial conformational adaptations of peptide antigens can contribute to antibody specificity. The experimental system consists of monoclonal antibodies against peptides that are closely sequence-related but adopt very different conformations in solution. The principle is shown schematically in Figure 1. Peptide antigens were designed that either fold into a well-ordered and stable coiled coil conformation or adopt an open chain, random coil structure. The switch between the ordered and the random coil conformation was achieved by substitution of two residues of a 29-residue coiled coil by Pro (Leder et al., 1994). A coiled coil consists of two (or more) peptides in an approximately α-helical conformation wound around

† This work was supported in part by the Swiss National Science Foundation (#31-36149.92), the Kommission für wissenschaftliche Forschung (KWF #2690.1), the Ciba-Geigy Jubiläums-Stiftung, the EMDO-Stiftung, and the Hartmann-Müller Stiftung.

* Corresponding author. Fax: +41 1 363 7947. E-mail: hrboss@bioc.unizh.ch.

‡ Present address: Department of Biological Chemistry and Molecular Pharmacology, Harvard Medical School, 240 Longwood Ave, Boston, MA 02115, U.S.A.

⊗ Abstract published in *Advance ACS Abstracts,* November 15, 1995.

0006-2960/95/0434-16509$09.00/0

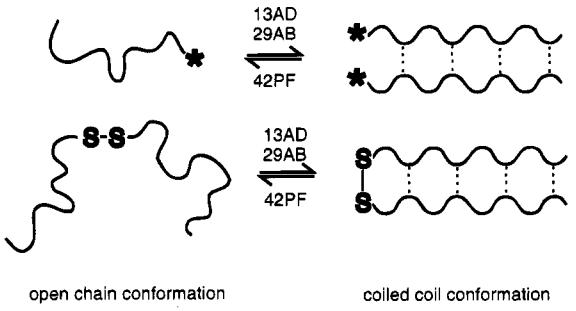

FIGURE 1: Illustration of the formation of a noncovalent coiled coil by association of monomeric peptides (top) and of the formation of a covalent coiled coil by the folding of disulfide-linked peptides (bottom). Monoclonal antibodies 13AD and 29AB shifted the conformational equilibrium in the direction of the coiled coil conformation. Monoclonal antibody 42PF shifted the equilibrium in the direction of the random coil conformation. Dots = hydrophobic interactions in the coiled coil conformation; asterisk = N- or C-terminal fluorescent label (Daca[2].)

each other, and the structure is formed by the concurrent association and folding of random coil monomers (Thompson et al., 1993). A coiled coil is built from repeating seven-residue motifs (*abcdefg*) in which Leu, Val, and Ile are frequent in *a* and *d* positions and form a hydrophobic interface between the strands of the coiled coil (Alber, 1992). Two types of antigenic coiled coil peptides were designed. In the first, formation of the coiled coil occurred by intermolecular association of monomeric peptides, in the second by intramolecular folding of two disulfide-linked peptides (Figure 1).

Monoclonal antibodies were produced against a coiled coil and a random coil peptide, and the cross-reactivity of the antibodies with the corresponding noncognate[1] peptides was evaluated by spectroscopic, microcalorimetric, and kinetic measurements. The influence of the antibodies on the open-closed equilibrium of the disulfide-linked peptides was followed by CD difference spectroscopy. Antibody-governed association and dissociation of the coiled coil was assessed by fluorescence quenching experiments on peptides with a terminal fluorescence group (marked by an asterisk in Figure 1), the emission of which was quenched in the coiled coil. The spectroscopic data demonstrated that the antibodies force the noncognate antigen to adopt a conformation that is similar to the conformation of the cognate antigen.

In principle, an antibody-induced conformational change may proceed in two ways. The conformational adjustment may take place within the antigen−antibody complex after the initial formation of a transitory encounter complex with a conformer of the peptide whose fit to the antibody binding site is not yet optimized. This mechanism conforms to Koshland's "classical" induced fit mechanism for enzyme−substrate reactions (Koshland et al., 1966). Alternatively, the antibody may select and bind a particular conformer of the peptide that fits to the antibody combining site and that is already present in solution before binding to the antibody occurs. From the very different rates observed here for the reaction of a monoclonal antibody with the cognate and noncognate peptide, respectively, a mechanism based on the conformational selection of a preexisting conformer of the antigen could be deduced.

[1] The peptide used to raise the monoclonal antibody is designated the cognate antigen or cognate peptide, and all other peptides are regarded as noncognate, irrespective of the degree of structural and conformational similarity to the cognate peptide.

MATERIALS AND METHODS

Peptide Synthesis and Purification. (See Table 1 for abbreviations of peptides.) Peptides were synthesized on an Applied Biosystems synthesizer model 430 A, using the Rapid Amide resin from DuPont and N^{α}-Fmoc[2] protection and carboxyl group activation by HBTU/DIPEA[2] as implemented by the instrument. The three consecutive terminal glycines were added as Fmoc-$(Gly)_3$ and cysteine as N^{α}-(Fmoc)-*S*-(*tert*-butylthio)cysteine. N-terminal Daca was introduced by reaction with a 2.5-fold excess of [7-dimethylaminocoumarin-(4)]acetic acid (Molecular Probes, Eugene, OR) in DMF, using HBTU/DIPEA activation. N-terminal biotin was introduced by reaction with a 5-fold excess of biotin-*p*-nitrophenylester (Fluka). C-terminal Daca was inserted by starting the synthesis with N^{α}-(Dde)-N^{ϵ}-(Fmoc)-lysine (Novabiochem, Läufelfingen, Switzerland). The N^{ϵ}-Fmoc group was removed and the product reacted with a 2.5-fold excess of [7-dimethylaminocoumarin-(4)]acetic acid by HBTU/DIPEA activation. The N^{α}-Dde group was removed by 2% hydrazine hydrate in DMF and the synthesis continued by the automated Fmoc/HBTU/DIPEA procedure. N^{α}-Acetylation was achieved by reaction of the resin-bound and side chain-protected peptide with acetic anhydride/triethylamine (2:1) in a 20-fold excess. Cleavage from the resin and deprotection of side chains, except *S*-(*tert*-butylthio)Cys, was achieved as before (Wendt et al., 1995). The *S*-*tert*-butylthio group was removed with a 100-fold excess of DTT in water for 20 h at 55 °C. After gel filtration on Sephadex G-25 in 1 M acetic acid (to remove excess DTT) and lyophilization, the peptide was dissolved in 0.1 M ammonium bicarbonate whereby the disulfide-linked peptide formed spontaneously by air oxidation. Peptides were purified by reversed-phase HPLC (Wendt et al., 1995), and their purity was checked by electrospray ionization mass spectrometry. Peptides were >95% pure. Peptide concentrations were determined by amino acid analysis.

A multiple antigenic peptide (Tam, 1988; Posnett & Tam, 1989) of LZ(7P14P) was prepared by automated stepwise synthesis of LZ(7P14P) onto a core of seven radially branching lysine residues attached to a polymeric carrier [Lys_4-Lys_2-Lys-Cys(Acm)-β-Ala Wang Resin; product 05-24-0151, Novabiochem], using Fmoc/HBTU/DIPEA chemistry. After deprotection and purification by high-performance liquid chromatography on a semipreparative C_8 column (Macherey-Nagel) eluted with a binary gradient of acetonitrile/H_2O containing 0.1% CF_3COOH, the free SH of Cys in [LZ(7P14P)]$_8$-Lys_4-Lys_2-Lys-Cys-β-Ala was reacted with *N*-iodoacetyl-*N*-biotinyl hexylenediamine (Pierce) to obtain the biotinylated multiple antigenic peptide. The correct mass of the product was confirmed by mass spectrometry.

Monoclonal Antibodies. Monoclonal antibodies 13AD and 29AB were obtained from two Balb/c mice that had been

[2] Abbreviations: Daca, [7-dimethylaminocoumarin-(4)]acetyl; Dde, 1-(4,4-dimethyl-2,6-dioxocyclohexyliden)ethyl; DIPEA, *N,N*-diisopropylethylamine; DMF, dimethylformamide; Fmoc, 9-fluorenylmethyloxycarbonyl; DTT, dithiothreitol; HBTU, O-benzotriazol-1-yl-*N,N,N',N'*-tetramethyluroniumhexafluorophosphate; ITC, isothermal titration calorimetry; PACE, protein A antibody-capture ELISA; PBS, phosphate-buffered saline; SPDP, *N*-succinimidyl-3-(2-pyridyldithio)propionate.

immunized with a Biotin-LZ_{SS}/avidin complex prepared by mixing Biotin-LZ_{SS} with avidin (Boehringer) at a molar ratio of 4.5:1. Subcutaneous injections of 100 μg of complex in complete Freund's adjuvant followed by four (13AD) or five (29AB) booster injections in incomplete adjuvant were applied. A last intraperitoneal injection of the antigen in PBS was applied 4 days before the mouse was killed, and the monoclonal antibodies were prepared according to standard techniques (Goding, 1986). Hybridomas were screened for the production of LZ-reactive antibodies with Biotinyl-LZ_{SS} bound to streptavidin-coated microwell plates. Monoclonal antibody 42PF was obtained from a Balb/c mouse that had been inoculated according to the above protocol (four booster injections) with the biotinylated multiple antigenic peptide/avidin complex (100 μg per inoculation). The last two inoculations were performed with 100 μg of Ac-Cys-LZ(7P14P) linked to keyhole limpet hemocyanin by reaction with SPDP (Pierce). The antigen was dissolved in PBS for the final inoculation. Hybridomas were screened for the production of LZ(7P14P)-reactive antibodies on microwell plates coated with Ac-Cys-LZ-(7P14P) linked to bovine serum albumin by reaction with SPDP. Milligram quantities of antibodies were produced from cells grown in roller bottles and purified on protein G (Pharmacia). Antibody concentration was determined from A_{280} (1 mg/mL) = 1.4 cm^{-1}.

Competition Enzyme Immunoassays. Details of the competition PACE have been published (Ngai et al., 1993). Briefly, microtiter plates (Nunclon MicroWell #1-67008A) were coated at 4 °C overnight with 50 μL/well of protein A (Pharmacia) dissolved (20 μg/mL) in coating buffer (15 mM Na_2CO_3, 34.8 mM $NaHCO_3$, 0.02% NaN_3, pH 9.6). Plates were washed with PBS/T (1.46 mM KH_2PO_4, 6.46 mM Na_2HPO_4, 0.14 M NaCl, 0.27 mM KCl, 0.02% NaN_3, 0.5% Tween-20, pH 7.2) and blocked with blocking buffer (2% fat-free dried milk in PBS/T) for 1 h at 37 °C. After being washed with PBS/T, plates were ready to capture the preformed antigen−antibody complex. This complex was prepared by incubation of biotinylated tracer antigen, serially diluted competitor antigen, and appropriately diluted antibody, for 1 h at room temperature. Tracer antigens were Biotin-LZ_{SS} for assaying 13AD and 29AB, and Biotin-LZ-$(7P14P)_{SS}$ for 42PF. The antibody dilution was chosen so that, in the absence of competitor, 60−80% of maximum absorbance was reached. Solutions were transferred to the protein A-coated microtiter plate and incubated for 1 h at 37 °C. Plates were washed with PBS/T and developed with streptavidin−alkaline phosphatase conjugate (Boehringer) and *p*-nitrophenylphosphate as substrate. Control assays performed with an unrelated antibody, with preimmune serum, or without second antibody were negative, as was the control reaction of the antibodies with streptavidin bound to the microtiter plate.

CD Spectroscopy. CD spectra were measured on a JASCO J-500 C spectropolarimeter at 20 °C and at a scan speed of 1 nm/min. Urea denaturation curves were measured at a constant wavelength of 222 nm in cuvettes of 2 mm path length as described before (Wendt et al., 1995). The denaturation curves for $LZ(16A)_{SS}$ and $LZ(14P)_{SS}$ were analyzed for the two-state equilibrium

$$U \rightleftarrows F \tag{1}$$

where U is the fraction of peptide in the open chain conformation and F the fraction in the coiled coil conformation (Figure 1, lower part). U and F were obtained from

$$U = 1 - \Delta\theta/\Delta\theta_{max} \tag{2a}$$

$$F = \Delta\theta/\Delta\theta_{max} \tag{2b}$$

$\Delta\theta = \theta - \theta_0$, where θ is the measured mean residue ellipticity and θ_0 is the mean residue ellipticity of the open chain conformation. $\theta_{0(222\ nm)} = -1500$ deg cm^2 $dmol^{-1}$ was obtained from the CD spectrum of $LZ(14P)_{SS}$ in 8 M urea. $\Delta\theta_{max} = \theta_{max} - \theta_0$, where θ_{max} is the mean residue ellipticity of the coiled coil conformation. A correction was made for the linear dependence of θ_{max} on urea concentration in the initial part of the unfolding curves (Pace et al., 1989; Jackson et al., 1993). The free energy of unfolding, ΔG_U, is given by

$$K_U = U/F = \exp(-\Delta G_U/RT) \tag{3}$$

The free energy change on unfolding in water, $\Delta G_U{}^W$, was extrapolated from the linear relationship (Pace et al., 1989)

$$\Delta G_U = \Delta G_U{}^W - m[\text{urea}] \tag{4}$$

CD titrations of antibodies with peptides were performed as follows: 1.2 mL of 1.2−2 μM antibody solution was placed in the cuvette, and the CD spectrum was measured in the range 205−240 nm. Thereafter, serial additions of 5−15 μL of 160−300 μM peptide stock solution were made. Three repetitive spectra were measured after each addition of peptide, and the spectra were corrected for dilution. Difference spectra were calculated by subtraction of the spectrum of the antibody from the spectra of the antigen−antibody complexes. In some experiments, the signal to noise ratio was large because of the strong CD absorption of the antibody.

Fluorescence Spectra. A Spex Fluorolog spectrofluorimeter was employed, and cuvettes of 1 cm path length were used. Spectra were measured at 25 °C in 1 nm steps with 2 s integration time. 1.8 mL of 2 μM Daca-labeled peptide was placed in the cuvette, and the fluorescence spectrum from 400 to 600 nm (excitation 380 nm) was measured in the presence of increasing amounts of monoclonal antibody added in 20 μL aliquots from 10−16 μM antibody stock solutions. The emmission maximum of peptides with an N-terminal Daca group was at 472 nm, that of peptides with a C-terminal Daca group at 478 nm. Spectra were corrected for dilution.

Stopped Flow Measurements. These were made at 25 °C on an SF-61 stopped flow spectrofluorimeter (High Tech Scientific Ltd., Salisbury, U.K.) as described previously (Wendt et al., 1995). Equal volumes of antibody and peptide solutions were mixed, and the change of fluorescence of the Daca-group was followed above 455 nm (cut-off filter OG455). Concentrations of antibody binding sites (2−20 μM) were always at least 4 times higher than those of the peptide (0.5−2 μM).

Buffers. ITC- and competition PACE were performed in PBS, pH 7.2, and spectroscopic and kinetic experiments in 0.1 M sodium phosphate buffer, pH 7.0.

RESULTS

Peptide Antigens. Table 1 lists the peptides and peptide derivatives used in this study. The first set consisted of

Table 1: Sequence of Antigenic Peptides

peptide	sequence [a]
	1 10 20
LZ	R_1-EYEALEKKLAALEAKLQALEKKLEALEHG-R_2
LZ(14P)	.....P.....
LZ(7P14P)	.....P.....P.....
LZ(16A)	.....A.....

[a] R_1 = N^{α}-acetyl, R_2 = amide, abbreviation = LZ, etc.; R_1 = N^{α}-acetyl-CGGG, R_2 = amide, abbreviation = LZ_{SS}, etc.; R_1 = biotinyl-GGG, R_2 = amide, abbreviation = Biotin-LZ, etc.; R_1 = biotinyl-GGGCGGG, R_2 = amide, abbreviation = Biotin-LZ_{SS}, etc.; R_1 = N^{α}-[7-dimethylaminocoumarin-(4)]acetyl-GGG, R_2 = amide, abbreviation = Daca-LZ, etc.; R_1 = N^{α}-acetyl, R_2 = GK(Daca)-amide, where K(Daca) is N^{ϵ}-[7-dimethylaminocoumarin-(4)]acetyllysine, abbreviation = LZ-Daca, etc.

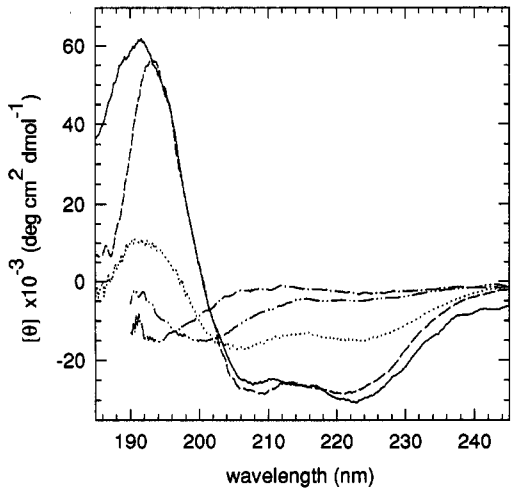

FIGURE 2: CD spectra of antigenic peptides in 0.1 M sodium phosphate buffer, pH 7.2, 20 °C, peptide concentration 27 μM. The mean residue ellipticity $[\theta]$ of the disulfide-linked peptides LZ_{SS} (- - -) and $LZ(7P14P)_{SS}$ (— •• —) is independent of the peptide concentration; $[\theta]$ of the nondisulfide-linked peptides LZ (—), LZ-(7P14P) (— • —), and LZ(14P) (• • •) is concentration dependent.

monomeric peptides that could associate to noncovalent dimeric and trimeric coiled coils. The second set included disulfide-linked peptides that could assume an open chain conformation as well as an ordered, coiled coil conformation (Figure 1). The N-terminal cystine of the covalent dimers was separated from the coiled coil part by triglycine spacers to prevent interference of the disulfide bond with the folding of the coiled coil part. The CD spectra of peptides LZ and LZ_{SS} (Figure 2) were characteristic of a coiled coil (Hodges et al., 1988; O'Shea et al., 1989). The spectra of LZ(7P14P) and $LZ(7P14P)_{SS}$ had the features of a mainly random coil structure (Figure 2). The mean residue ellipticity of the disulfide-linked peptides was independent of the peptide concentration (data not shown). The CD spectrum of the nondisulfide-linked peptides was concentration dependent, in accord with a monomer/coiled coil equilibrium (Figure 3B).

LZ_{SS} formed an extremely stable coiled coil as demonstrated by the urea unfolding curve in Figure 3A. Substitution of Leu-16 by Ala, or of Ala-14 by Pro, destabilized the coiled coil (O'Neil & DeGrado, 1990; Zhou et al., 1992; Wendt et al., 1995). The urea unfolding curves of Figure 3A were analyzed for a two-state equilibrium between an

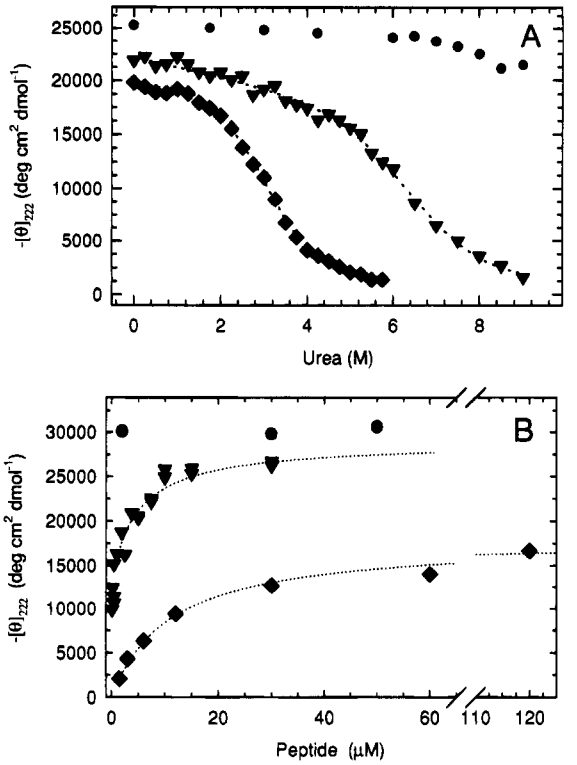

FIGURE 3: (A) Urea denaturation of disulfide-linked peptide LZ_{SS} (●), $LZ(16A)_{SS}$ (▼), and $LZ(14P)_{SS}$ (◆). Dotted lines are best fits to a concentration-independent two-state equilibrium between an open conformation and a closed coiled coil conformation (see Materials and Methods for details of fitting procedure). (B) Concentration dependence of $[\theta]_{222}$ of nondisulfide-linked peptides LZ (●), LZ(16A) (▼), and LZ(14P) (◆). The dotted line through the data points for LZ(16A) is a best fit to the sum of two hyperbola. The extrapolated maximum $[\theta]_{222}$ at infinite concentration is $-28\,900$ deg cm^2 dmol^{-1}. The data points for LZ(14P) were analyzed for a monomer/dimer equilibrium as described by Wendt et al. (1995); the dotted line is a best fit for $K_d = 21.6 \pm 3.6$ μM and maximum $[\theta]_{222} = -17\,950$ deg cm^2 dmol^{-1}.

open chain conformation and a closed coiled coil conformation to obtain the free energy of unfolding, ΔG_U^W, listed in Table 2. The shape of the curves and the position of their midpoints indicated that $LZ(16A)_{SS}$ and $LZ(14P)_{SS}$ were in the closed coiled coil conformation when in aqueous buffer. It should be noted that the mean residue ellipticity in aqueous buffer became less negative with decreasing coiled coil stability, which has been interpreted as a reflection of a nonideal α-helical structure of a coiled coil that contains a Leu to Ala substition at the hydrophobic interface or a Pro in a surface-exposed position (Wendt et al., 1995).

Figure 3B shows the concentration dependence of $[\theta]_{222}$ of the nondisulfide-linked peptides LZ, LZ(16A), and LZ-(14P). $[\theta]_{222}$ of LZ was concentration-independent in the range 1−50 μM, a decrease of $[\theta]_{222}$ being observed only well below micromolar peptide concentration (H.W., unpublished results). Indeed, LZ forms a very stable trimeric, parallel coiled coil (Wendt et al., 1995). The monomer/coiled coil equilibrium of peptides LZ(16A) and LZ(14P) varied in the concentration range used in the present experiments. Peptide LZ(16A) forms dimers and trimers. We have shown before that monomers and dimers dominate at low concentrations and trimers are formed at higher concentrations (Wendt et al., 1995; Thomas et al., 1995). In sedimentation equilibrium analysis, 7 μM LZ(16A) exhibited an apparent mass of 5700 ± 110 Da, corresponding to 87%

Table 2: Free Energy of Unfolding, Midpoint Concentration of Urea Unfolding Curves, and C_{50} Concentrations for Competition Enzyme Immunoassay

peptide[a]	ΔG_U^{W} [b] (kJ/mol)	$urea_{50}$[c] (mol/L)	C_{50} of competition PACE[d] mAb 13AD	mAb 29AB	mAb 42PF
LZ_{SS}	nd[f]	>9	0.8	0.6	30
LZ	33.6 ± 0.3[e]	6.7	1	0.6	20
$LZ(16A)_{SS}$	23.6 ± 0.9	6.8	1.5	7	1
$LZ(14P)_{SS}$	11.7 ± 0.2	3.0	2	5	0.2
$LZ(7P14P)_{SS}$	na[f]	na	15	15	0.1
LZ(7P14P)	na	na	60	>100	0.3

[a] Sequence and abbreviation of peptides in Table 1. [b] Free energy of unfolding in water per peptide chain, calculated from the urea denaturation curve by the linear extrapolation method (see Materials and Methods). [c] Concentration of urea, estimated from the urea unfolding curve, at which the CD signal at 222 nm dropped to 50% of the initial value in water. [d] C_{50} is the micromolar concentration of peptide necessary to reduce the binding of Biotin-LZ_{SS} to antibody 13AD and 29AB or of Biotin-$LZ(7P14P)_{SS}$ to antibody 42PF, by 50%. Assays were performed with 0.28 μM 13AD, 0.07 μM 29AB, or 0.27 μM 42PF; the biotinylated tracer antigen was 0.3 μM and the competitor antigen varied from 0 to 200 μM. See Materials and Methods for details of the immunoassay. [e] Eberhard Dürr, unpublished experiment. [f] nd, not determined; na, not applicable.

of the calculated dimer mass (Wendt et al., 1995). This mass and the concurring $[\theta]_{222}$ of −24 000 deg cm^2 dmol^{-1}, which is 80% of the maximum $[\theta]$ at infinite peptide concentration (Figure 3B), indicated that the concentration of trimer was small in 7 μM LZ(16A).[3] LZ(14P) associated to a dimeric coiled coil in the concentration range tested. The data shown in Figure 3B fit to a monomer/dimer equilibrium with K_d = 21.6 ± 3.6 μM. The ellipticity of LZ(16A) and LZ(14P) extrapolated to infinite peptide concentration is less negative than in the three-stranded coiled coil LZ.

Production of Monoclonal Antibodies. Immunization was effected with the disulfide-linked peptide Biotin-LZ_{SS} coupled to avidin as a carrier to ensure that the coiled coil conformation of LZ remained intact. In Biotin-LZ_{SS}, a triglycine spacer was introduced between the disulfide bond and the biotin group to facilitate the access of the biotin group to the binding cavity of avidin. About a dozen LZ-specific monoclonal antibodies were obtained from two fusion experiments, and antibodies 13AD (IgG1) and 29AB (IgG2a) were chosen for further studies.

Initial attempts to obtain high titer antibodies against LZ(7P14P) by immunization with the peptide coupled to keyhole limpet hemocyanin were unsuccessful, only antibodies of the IgM class being produced. Eventually, antibody 42PF was obtained after immunization with a multiple antigenic peptide composed of 8×LZ(7P14P) grafted onto a seven-lysine core (Tam, 1988).

Competition Enzyme Immunoassay. Antibody specificity for antigens differing primarily in conformation must be tested in a solution-phase immunoassay because antigen and antibody may denature in a solid-phase assay due to adsorption to the plastic surface of the microtiter plate (Spangler, 1991; Schwab & Bosshard, 1992). We have developed a conformation-sensitive protein A antibody-capture ELISA (Ngai et al., 1993) in which the antigen−antibody reaction takes place in solution and only the quantification of bound antigen is performed on the microtiter plate (see Materials and Methods). The disulfide-linked peptides had to be used as competitor antigens because the conformational equilibrium of the nondisulfide-linked peptides changed in the concentration range of the competition assays except in the case of the fully unfolded LZ(7P14P) and the fully folded trimeric coiled coil LZ. Table 2 shows values of C_{50}, the concentration of competitor antigen necessary to reduce the binding of the tracer antigen to the antibody by 50%. As expected, the cognate antigen was the best competitor (lowest C_{50}). The degree of competition approximately reflected the stability of the coiled coil conformation of the noncognate peptides: LZ(7P14P) and $LZ(7P14P)_{SS}$ competed more weakly for antibodies 13AD and 29AB, and LZ and LZ_{SS} more weakly for antibody 42PF. Competition by peptides $LZ(16A)_{SS}$ and $LZ(14P)_{SS}$ was intermediate between that of the most stable and the least stable coiled coil. Antibodies 13AD and 29AB did not react to any significant extent with the overlapping synthetic peptides corresponding to LZ sequences 1−10, 6−15, 11−20, 16−25, and 20−29, from which it followed that the epitopes recognized by the two antibodies depended on a conformation that was only formed by the intact peptide (data not shown). Antibody 42PF reacted with LZ peptide 11−20 and was therefore probably directed against a sequential epitope in this region of the cognate peptide LZ(7P14P) (not shown).

Antibody Binding Changes Conformation of Noncognate Peptide. Changes in the CD spectrum were analyzed by titration of the antibodies with the different cognate and noncognate peptides. Titration of 29AB with cognate LZ and LZ_{SS} produced no measurable change in the CD. Similarly, no CD change was observed on titration of 42PF with cognate LZ(7P14P) and $LZ(7P14P)_{SS}$. In contrast, binding of the noncognate peptides was accompanied by significant changes in the far-UV CD spectrum (Figure 4). The significant noise in some spectra of Figure 4 is caused by the large CD absorption of the free antibody as compared to the relatively small amplitudes of the spectral changes. The top panels of Figure 4 show two examples of the titration of antibody 29AB with noncognate peptides. Binding of LZ(14P) or $LZ(7P14P)_{SS}$ to 29AB induced a strong negative ellipticity at 229 nm and a weaker positive ellipticity at 216 nm. Essentially the same results were obtained with the other noncognate peptides whether or not they were disulfide-linked or had a N-terminal Daca fluorescence label. The changes could have been caused by conformational changes in the noncognate peptide as well as in the antibody. The negative band centered at 229 nm could originate from the formation of a coiled coil-like structure although the position of the band is rather high, the characteristics of an α-helical structure being two minima at approximately 222 and 208 nm. The positive band at 216 nm could reflect a small change of structure of the antibody. (The antibody spectrum exhibits a very strong negative band around 215 nm because of the high β-sheet content of antibodies.) Furthermore, the positive bands at 216 nm in the upper panels of Figure 4 could have concealed the formation of the second minimum typical for α-helical structure. We conclude that induction

[3] The mean residue ellipticity of the monomer is close to zero (Wendt et al., 1995; Betz et al., 1995), and the mean residue ellipticity of dimer and trimer can be assumed to be equal (Betz et al., 1995). From this one concludes that, since $[\theta]_{222}$ accounted for 80% of the maximum mean residue ellipticity, the apparent mass of LZ(16A) in a 7 μM solution would have been well above the mass of the dimer if trimers had dominated over dimers.

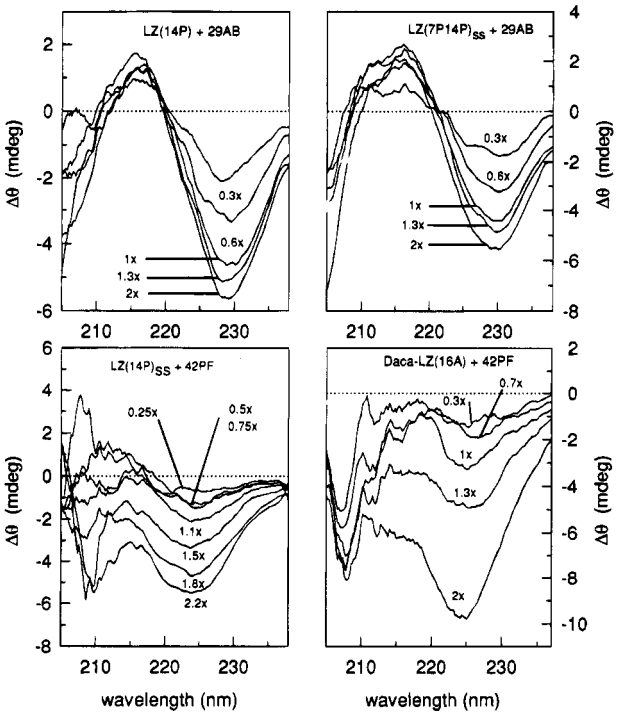

FIGURE 4: CD spectrum of noncognate peptide changes on binding to monoclonal antibody. A fixed amount of antibody was titrated with increasing amounts of noncognate peptide. CD difference spectra were obtained by subtracting the spectrum of the free antibody from the spectrum of peptide−antibody mixture. The ratio of peptide to antibody site is indicated for each spectrum by 0.3×, 0.6×, etc. Binding of LZ(14P) and $LZ(7P14P)_{SS}$ to antibody 29AB induces a negative band centered at 229 nm and a positive band at 216 nm (top panels). Binding of $LZ(14P)_{SS}$ and Daca-LZ(16A) to antibody 42PF reduces the negative ellipticity centerd at 225 nm (bottom panels). Concentration of antibody sites: 2.8 μM 29AB (top panels), 2.6 μM 42PF (bottom left), and 4 μM 42PF (bottom right).

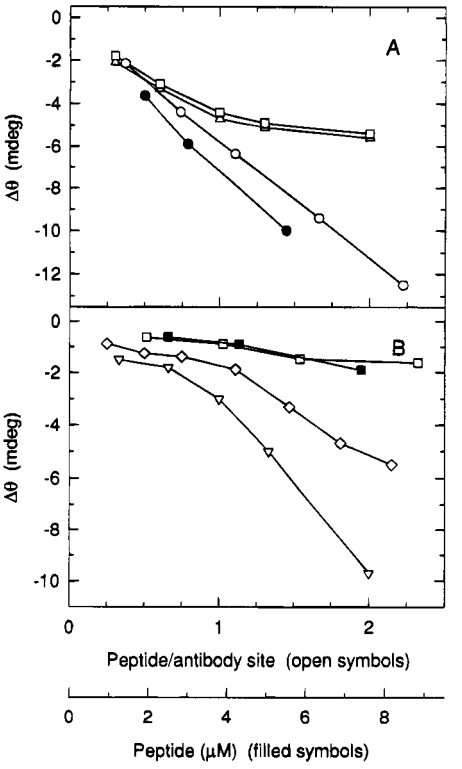

FIGURE 5: Change of ellipticity at minimum of CD difference spectrum with increasing ratio of peptide to antibody site. (A) Binding of LZ(14P) (△) and $LZ(7P14P)_{SS}$ (□) to antibody 29AB. $\Delta\theta$ refers to the minimum at 229 of the CD difference spectrum in the top panels of Figure 4. As a control, the steep linear decrease of $\Delta\theta$ on addition of cognate LZ_{SS} in the presence (○) and absence (●) of 29AB is shown. (B) Binding of $LZ(14P)_{SS}$ (◇) and Daca-LZ(16A) (▽) to antibody 42PF. $\Delta\theta$ refers to the minimum at 225 nm of the difference CD spectrum in the bottom panels of Figure 4. As a control, the small linear decrease of $\Delta\theta$ on addition of cognate $LZ(7P14P)_{SS}$ in the presence (□) and absence (■) of 42PF is shown. In panels A and B, the slopes of the lines of the noncognate peptides change after the addition of approximately one peptide chain per antibody binding site, in accordance with a 1:1 stoichiometry.

of a helix-like conformation seems a sensible interpretation of the CD difference spectra, particularly so since in the immunoassays only the intact 29-residue peptides were recognized (see above).

The situation is simpler for antibody 42PF. Two examples of CD titration experiments are shown in the bottom panels of Figure 4. Binding of the noncognate peptides $LZ(14P)_{SS}$ and Daca-LZ(16A) to 42PF reduced the ellipticity around 225 nm, a clear indication of a lowered helix content forced upon these peptides when they bound to 42PF. A qualitatively similar result was obtained with $LZ(16A)_{SS}$. Binding of LZ_{SS} to 42PF could not be measured because the cross-reactivity was quite weak and the reaction very slow (see below).

In Figure 5, $\Delta\theta$ at the minimum of the CD difference spectra of Figure 4 is plotted against the peptide/antibody site ratio. The titration curves for the noncognate peptides are nonlinear. The slope changes at approximately one peptide per antibody binding site. The initial slope of the titration with 29AB approached the slope of the control titration with the cognate peptide LZ_{SS} (panel A). Similarly, the initial slope of the titration with 42PF was similar to that of the control titration with cognate $LZ(7P14P)_{SS}$ (panel B). These observations are in accord with the possible induction of a coiled coil-like structure by 29AB and with the unfolding of the coiled coil structure by 42PF.

Antibodies Change the Position of the Monomer/Coiled Coil Equilibrium of Noncognate Peptides. To demonstrate that the antibodies can change the equilibrium position between monomeric peptide chains and noncovalent coiled coils, fluorescence titration experiments were performed with the nondisulfide-linked peptides containing a Daca group at the N- or C-terminal end. The experiments relied on our previous observation that the emission of a fluorescent group attached to the N- or C-terminus of a coiled coil is weak because of mutual quenching of the adjacent fluorophores in a parallel coiled coil (Wendt et al., 1994). The Daca group, attached via a triglycine spacer, does not significantly interfer with the monomer/coiled coil equilibrium (Wendt et al., 1994, 1995). If antibody 13AD and 29AB force a predominantly monomeric peptide to associate into a coiled coil, the fluorescence of the Daca group must decrease. This was indeed the case as is shown in the upper panel of Figure 6 for the titration of Daca-LZ(7P14P) with 29AB. The decrease in fluorescence as a function of antigen concentration leveled out at one peptide chain per antibody binding site, in accordance with the stoichiometry seen in the CD-titration experiment (Figure 5). The fluorescence decrease was smaller when Daca-LZ(14P) was titrated with 29AB because, under the conditions of the experiment, a fraction of Daca-LZ(14P) was present as a coiled coil before antibody 29AB was added (Figure 3B). No fluorescence change was

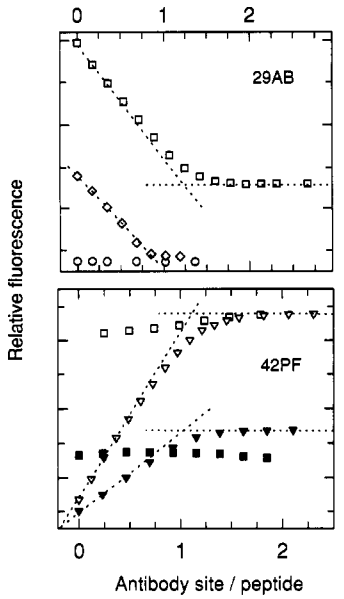

FIGURE 6: Fluorescence titration of Daca-labeled peptides with antibody 29AB (top) and 42PF (bottom). 2.0 μM peptide was titrated at 25 °C with antibody, and the fluorescence was measured at the emission maximum (see Materials and Methods). Daca-LZ (○), Daca-LZ(14P) (◇), Daca-LZ(16A) (▽), LZ(16A)-Daca (▼), Daca-LZ(7P14P) (□), LZ(7P14P)-Daca (■).

seen in the control titration of coiled coil Daca-LZ with 29AB. The fluorescence signal at antibody saturation was higher for Daca-LZ(7P14P) than for Daca-LZ and Daca-LZ-(14P), probably because the two Pro in LZ(7P14P) prevented the formation of a perfect coiled coil in which the Daca groups were sufficiently close to be as strongly quenched as in Daca-LZ.

Complementary results were obtained with antibody 42PF that induced dissociation in Daca-LZ(16A) (Figure 6, lower panel).[4] Dissociation of Daca-LZ could also be demonstrated, but the data were more scattered because a complete titration experiment lasted almost 2 days due to the very slow binding of Daca-LZ to antibody 42PF (see below). To prove that the fluorescence change reflected the dissociation of the coiled coil and was not caused by direct interaction of the Daca group with the antibody binding site (which might happen, for example, if Daca were part of the epitope), titrations were repeated with peptides LZ(16A)-Daca and LZ-(7P14P)-Daca in which the fluorescent group was at the C-terminus. The position of the fluorescent group had no influence on the outcome of the experiment.

Cross-Reaction with the Noncognate Peptides and Enthalpy/Entropy Compensation. The energetics of peptide binding by the three antibodies was measured by ITC, which, in a single experiment, provides the enthalpy of binding ΔH, the association constant K_a, and the stoichiometry N of the antigen−antibody complex (Wiseman et al., 1989; Jelesarov et al., 1995). The free energy and the entropy of the complex were calculated from $\Delta G = RT \ln K_a$; $T\Delta S = \Delta H - \Delta G$. Thermodynamic parameters of the reaction of 13AD and 29AB with LZ, LZ_{SS}, LZ(7P14P), and $LZ(7P14P)_{SS}$ are shown in Table 3. Parameters of the reaction of 42PF with cognate LZ(7P14P) and $LZ(7P14P)_{SS}$ and noncognate $LZ-(14P)_{SS}$ are shown in Table 4. Binding by 42PF of noncognate LZ_{SS} and LZ could not be measured by ITC because the heat of reaction was too small. The stoichiometries deduced from the ITC experiments were in the range 0.8−1.1 peptide chain per antibody binding site. Disulfide-linked peptides were counted as two peptide chains, i.e., the stoichiometry was two antibody binding sites per LZ_{SS} and its derivatives.

The comparison of ΔH and $T\Delta S$ in columns 2, 3 and 6, 7 of Table 3 revealed that the modest difference in K_a for the reactions of 13AD and 29AB with LZ and LZ(7P14P), respectively, was due to large enthalpy/entropy compensation. This is best demonstrated by the values of $\Delta\Delta E$[5] calculated from Table 3. Binding of noncognate LZ(7P14P) to 13AD was enthalpically favored by $\Delta\Delta H = -19.8$ kJ/mol and entropically disfavored by $T\Delta\Delta S = -23.8$ kJ/mol. The corresponding energy differences for the reaction of 29AB with LZ and LZ(7P14P) were $\Delta\Delta H = -13.6$ kJ/mol and $T\Delta\Delta S = -20.5$ kJ/mol. Enthalpy/entropy compensation was much less pronounced in the case of the reaction with the disulfide-linked cognate and noncognate peptides (columns 4, 5 and 8, 9 of Table 3).

The situation was reversed for antibody 42PF (Table 4). The strong cross-reaction with the noncognate peptide $LZ-(14P)_{SS}$ was again enabled by enthalpy/entropy compensation, but $\Delta\Delta H$ was now unfavorable (positive) and $T\Delta\Delta S$ favorable (positive). Values of $\Delta\Delta E$ for the pair $LZ(7P14P)_{SS}$ and $LZ(14P)_{SS}$ were $\Delta\Delta H = +24.2$ kJ/mol and $T\Delta\Delta S = +20.5$ kJ/mol.

Enthalpy changes at 17, 27, and 37 °C depended linearly on temperature (not shown). The measured heat capacity changes, ΔC_P, corresponding to the slope $d\Delta H/dT$, are listed in Tables 3 and 4. ΔC_P values were large and negative, which is typical for a reaction in which hydrophobic surface is buried. The reaction of 13AD and 29AB with the noncognate peptide LZ(7P14P) had a more negative ΔC_P than the reaction with the cognate peptide LZ. In contrast, ΔC_P was less negative when 42PF reacted with noncognate $LZ(14P)_{SS}$.

Reactions with Noncognate Peptides Are Much Slower Than with Cognate Peptides. Figure 7 shows the time course of several noncognate reactions monitored from the change of fluorescence of the Daca group. The apparent half-times of the reaction of antibody 42PF with Daca-LZ and Daca-LZ(16A) differed by more than 100-fold (right panel of Figure 7). Moreover, $t_{1/2}$ was independent of the total peptide concentration in the presence of excess antibody (2−20 μM antibody binding site, 0.5−2 μM peptide). This indicated that the dissociation of the coiled coil was rate-limiting for the reaction with 42PF. Indeed, $t_{1/2}$ of the antibody reaction and of the concentration-independent dissociation of the coiled coil were of the same order of magnitude with $t_{1/2} = 930$ s for antibody binding to Daca-LZ and $t_{1/2} = 2000$ s for strand dissociation (Wendt et al., 1995). The corresponding $t_{1/2}$ values for Daca-LZ(16A) were 7 s for antibody binding

[4] Titration with 42PF of peptide $LZ(16A)-Daca_{SS}$, which has a N-terminal disulfide bond and two C-terminal Daca groups, also led to an increase of fluorescence saturating at one peptide chain per antibody site. This further demonstrated that 42PF shifts the conformational equilibrium to the side of the open chain conformation (Figure 1, lower panel), in support of the CD data shown for other disulfide-linked peptides in Figure 4.

[5] $\Delta\Delta E$ is defined as $\Delta E_{noncognate} - \Delta E_{cognate}$, where E stands for either enthalpy, entropy, or free energy.

Table 3: Thermodynamic Parameters of Binding of Monoclonal Antibodies 13AD and 29AB to Cognate and Noncognate Peptide Antigen[a]

	antibody 13AD				antibody 29AB			
	LZ	LZ(7P14P)	LZ_{SS}	$LZ(7P14P)_{SS}$	LZ	LZ(7P14P)	LZ_{SS}	$LZ(7P14P)_{SS}$
ΔG	-43.9 ± 0.7	-39.9 ± 0.6	-42.5 ± 2.1	-42.3 ± 1.1	-45.9 ± 1.6	-39.9 ± 1.6	-44.6 ± 1.4	-42.6 ± 0.4
ΔH	-52.8 ± 0.7	-72.6 ± 1.1	-51.1 ± 0.6	-56.7 ± 1.5	-57.8 ± 1.4	-71.4 ± 2.7	-59.8 ± 2.3	-59.5 ± 0.8
$T\Delta S$	-8.9 ± 1.4	-32.7 ± 1.6	-8.6 ± 2.7	-14.4 ± 2.6	-11.9 ± 3.0	-32.4 ± 4.3	-15.3 ± 3.8	-16.9 ± 1.2
$K_A \times 10^{-7}$ (M^{-1})	4.5 ± 1.1	0.9 ± 0.2	2.5 ± 1.4	2.3 ± 0.8	9.7 ± 4.5	0.6 ± 0.3	5.7 ± 2.5	2.6 ± 0.4
ΔC_P	-1.05	-1.53	nd	nd	-1.40	-1.64	nd	nd

[a] ITC measurements were made as described by Jelesarov and Bosshard (1994). ΔG, ΔH, and $T\Delta S \pm$ SD are in kJ mol^{-1} at 27 °C; ΔC_P in kJ mol^{-1} K^{-1}.

Table 4: Thermodynamic Parameters of Binding of Monoclonal Antibody 42PF to Cognate and Noncognate Peptide Antigen[a]

	antibody 42PF		
	LZ(7P14P)	$LZ(7P14P)_{SS}$	$LZ(14P)_{SS}$
ΔG	-43.5 ± 1.5	-42.0 ± 1.5	-38.3 ± 2.2
ΔH	-56.0 ± 1.9	-58.5 ± 3.6	-34.3 ± 2.2
$T\Delta S$	-12.5 ± 3.4	-16.5 ± 5.1	4.0 ± 4.4
$K_A \times 10^{-7}$(M^{-1})	3.8 ± 1.8	2.1 ± 1.0	0.5 ± 0.3
ΔC_P	-2.89	nd	-1.86

[a] ΔG, ΔH, and $T\Delta S \pm$ SD are in kJ mol^{-1} at 27 °C; ΔC_P in kJ mol^{-1} K^{-1}.

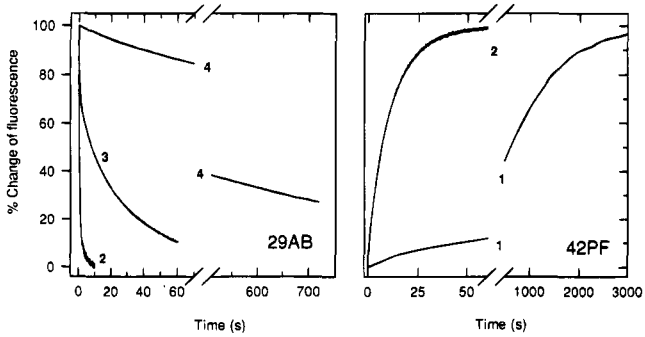

FIGURE 7: Time course of the reaction of monoclonal antibodies with cognate and noncognate peptides. Rates are slower the more "noncognate" the peptide. (Left) Reaction of antibody 29AB (6 μM antibody binding site) with 0.3 μM peptides. (Right) Reaction of antibody 42PF (6 μM antibody binding site) with 0.5 μM peptides. 1 = Daca-LZ, 2 = Daca-LZ(16A), 3 = Daca-LZ(14P), 4 = Daca-LZ(7P14P).

and 5 s for strand dissociation (Wendt et al., 1995).[6] The rate of reaction of antibody 29AB with Daca-LZ(16A), Daca-LZ(14P), and Daca-LZ(7P14P) paralleled the propensity of these three noncognate antigens to form coiled coils (left panel of Figure 7). Daca-LZ(16A) reacted fastest, random coil Daca-LZ(7P14P) reacted slowest, and the rate with Daca-LZ(14P) was intermediate. The rates of reaction of an excess of 29AB (Figure 7) and of 13AD (not shown) depended on the concentration of the peptides, in contrast to the concentration-independent rates observed with 42PF.

DISCUSSION

Perhaps the earliest demonstration of an antibody-induced conformational change was the observation that an antiserum against apomyoglobin forced the heme out of methemoglobin (Crumpton, 1966). Today, our knowledge on the contribution of molecular flexibility to antibody specificity is based mainly on the comparison of a relatively small number of X-ray structures of antigen−antibody complexes and their free components. Small movements are evident in several protein−antibody complexes (Wilson & Stanfield, 1994; Braden & Poljak, 1995). Adjustments of the antigen conformation are more obvious when a peptide binds to an antibody. Short linear peptides are usually unstructured in aqueous solution, and an antipeptide antibody may constrain several residues of the peptide into an ordered conformation (Wilson & Stanfield, 1994). The most commonly seen structure of the part of the peptide contacting the antibody is a β-turn, which may or may not be a preferred conformer of the free peptide in aqueous solution (Shoham, 1993; Wilson & Stanfield, 1994; Dyson & Wright, 1995). Induction of helical structure in a peptide antigen has been described for at least one antipeptide antibody (Tsang et al., 1992).

Here we introduce coiled coil peptides as models for the study of conformational adaptation in peptide−antibody reactions in solution. LZ and LZ(7P14P) constitute a suitable peptide pair to explore conformation-dependent antibody cross-reactions as these peptides have very similar sequences yet very disparate conformations. Coiled coil peptide LZ, designed on a sequence originally used to probe the helix-forming propensity of amino acids (O'Neil & DeGrado, 1990), forms a three-stranded parallel coiled coil (Wendt et al., 1995; Thomas et al., 1995). The analogue LZ(7P14P) lacks helical structure in the CD spectrum (Leder et al., 1994), although it is not known if LZ(7P14P) is fully unfolded or has some residual nonhelical structure. The peptide may show conformational preferences in the multiple antigenic peptide that was used to elicit monoclonal antibody 42PF.

Conformational Adaptation of the Antigen Inferred from CD and Fluorescence Measurements. The CD difference spectra demonstrated the induction of very significant antibody-induced conformational changes in the noncognate peptides. The nature of the CD change points to the induction of helical structure by the anti-coiled coil antibodies 13AD and 29AB and to the disruption of helix by antibody 42PF. Unequivocal demonstration of helix induction was, however, not possible from the shape of the CD difference spectra. Antibody-promoted assembly and disassembly of the coiled coil structure was demonstrated by the fluorescence titration experiments. Together, the CD and fluorescence data imply that the antibody-bound noncognate peptides adopt a conformation that is similar to the conformation of the cognate peptide. It is improbable that the very substantial spectral changes accompanying the cross-reactions would have been observed if the antibodies had reacted with epitopes that were *a priori* present in the coiled coil and in the random coil conformation, for example, linear epitopes

[6] Strand dissociation was measured with fluorescein-labeled peptides (Wendt et al., 1995).

near the N- or C-termini accessible in the random coil as well as in the coiled coil conformation [the ends of a coiled coil tend to be frayed (Zhang & Hermans, 1993)]. Such a possibility can also be excluded on the basis of the competition immunoassay in which no cross-reaction with the N- and C-terminal decapeptides was observed.

The Energetic Cost of the Conformational Change Is Counterbalanced by Enthalpy/Entropy Compensation. Considering the values of ΔG_U^W of the coiled coil peptides (Table 2), folding or unfolding of the coiled coil on binding to the antibody would seem to be energetically very unfavorable. An explanation was found in an almost total enthalpy/entropy compensation. $\Delta\Delta H$ of the noncognate reaction of 13AD and 29AB was exothermic (negative) and $T\Delta\Delta S$ was unfavorable (negative). Is this observation in qualitative agreement with the energetics of the formation of a coiled coil? Folding of the leucine zipper domain of yeast transcription factor GCN4 is driven by negative ΔH and opposed by an unfavorable entropy change (Thompson et al., 1993). Similarly, we found that the folding of a heterodimeric coiled coil model peptide exhibited negative ΔH and negative $T\Delta S$ at 27 °C (I.J. and H.R.B., unpublished experiments). The formation of a coiled coil entails the burial of hydrophobic surface and the formation of directed hydrogen bonds. At least in the case of GCN4 and of our heterodimeric model coiled coil, the folding process is exothermic and the unfavorable $T\Delta\Delta S$ agrees with a loss of conformational and cratic entropy, which overcompensates a positive entropic contribution from the solvent effect, that is, from the loss of structured water on burial of hydrophobic surface. The signs of $\Delta\Delta H$ and $T\Delta\Delta S$ are reversed for the unfolding of a coiled coil, exactly as observed for the reaction of antibody 42PF with noncognate $LZ(14P)_{SS}$.

Our interpretation of the thermodynamic changes is also in qualitative agreement with the heat capacity changes for the cognate and noncognate reactions. First, ΔC_P is negative for the cognate reactions. A negative ΔC_P characterizes protein folding and association and has been interpreted as resulting in changes in water-accessible surface area and nonpolar surface (Sturtevant, 1977; Livingstone et al., 1991; Murphy & Freire, 1992). The values of ΔC_P in Tables 3 and 4 are of similar magnitude as those reported for other antigen−antibody reactions (Schwarz et al., 1995). A more negative ΔC_P for 42PF binding to LZ(7P14P) and a less negative ΔC_P for 13AD or 29AB binding to LZ make sense as the epitope on the open chain peptide LZ(7P14P) may involve more hydrophobic surface than the epitopes of 13AD and 29AB that are on the hydrophilic and charged surface of the intact coiled coil. Second, ΔC_P becomes more negative when 13AD and 29AB bind to the noncognate peptide. Provided that the structures of the cognate and noncognate antigen−antibody complex are similar, the more negative ΔC_P can be assigned to the burial of surface when LZ(7P14P) is forced into a coiled coil-like structure. By the same reasoning, the less negative ΔC_P for the reaction of 42PF with $LZ(14P)_{SS}$ could be caused by the antibody-induced opening of the coiled coil structure and the concomitant exposure of nonpolar surface.

In the absence of precise 3D structures of the antigen−antibody complexes with which to compare the thermodynamic parameters, the above interpretations must remain speculative. In particular, in assuming that the differences $\Delta\Delta H$, $T\Delta\Delta S$, and $\Delta\Delta C_P$ are caused mainly by changes in the antigen, possible conformational adjustments in the antibody are neglected. However, the internal consistency of $\Delta\Delta E$ values and the generally minor movements of the antibody conformation in antigen−antibody crystal structures (Wilson & Stanfield, 1994; Braden & Poljak, 1995) give credence to the interpretation of the thermodynamic parameters.

The Cross-Reactions Follow a Conformational Selection Mechanism. The reactions with the noncognate peptides can be represented by the scheme:

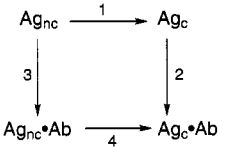

Ag_{nc} is the noncognate peptide, Ag_c is the same peptide in the cognate (or cognate-like) conformation, and Ab is the monoclonal antibody. A "classical" induced fit mechanism (Koshland et al., 1966) follows the path 3 → 4, that is, Ag_{nc}•Ab is formed initially, and the induced fit reaction occurs in step 4 when the peptide is already bound to the antibody. The alternative pathway 1 → 2 we call "induced fit by conformational selection". The antibody only binds to that conformer of the antigen that is already in the cognate (or cognate-like) conformation. Step 2 is slow if the concentration of Ag_c is small, as confirmed by the results in Figure 7. Rates were very much slower for peptides present in a mainly noncognate conformation and much faster for peptides in a mainly cognate conformation. This was particularly clear for antibody 42PF and is a very strong indication for pathway 1 → 2 with reaction 1 as the rate-limiting step. The situation is more complex for antibodies 13AD and 29AB. In a "classical" induced fit, these antibodies would have to react with two monomeric peptides LZ(7P14P) in step 3. Thereafter, the peptides would have to associate to a coiled coil while bound to the antibody, a rather implausible mechanism in comparison to the simpler selection mechanism 1 → 2 in which the antibody selects whatever small amount of coiled coil (or coiled coil-like) antigen is present in solution.

CONCLUSIONS

We have demonstrated that peptides may undergo large conformational changes on binding to a monoclonal antibody. The antibody-induced conformational adjustments, which are energetically unfavorable in the free peptides, are realized thanks to near complete enthalpy/entropy compensation. The very different rates of the cognate and noncognate reactions point to a conformational selection mechanism rather than to a "classical" induced fit within the antigen−antibody complex. A conformational selection mechanism allows for a surprisingly large "deformation" of the antigen structure without violation of the requirement for a precise preexisting fit between free antigen and antibody. It would seem that many antibody cross-reactions occur not because the antigen and antibody are particularly flexible and malleable but because the antibody selects a fitting conformer even if this constitutes only a very minor fraction. Antibodies produced deliberately against a conformational isomer, such as the destabilized coiled coil peptides used here, could be useful tools to specifically control biological processes.

ACKNOWLEDGMENT

We thank Toni Baici for allowing us to use his stopped-flow instrument and for help with the kinetic experiments, Eberhard Dürr for help with some urea unfolding experiments, and Richard M. Thomas for a critical reading of the manuscript.

REFERENCES

Alber, T. (1992) *Curr. Opin. Genet. Dev. 2*, 205−210.
Arnon, R., & Van Regenmortel, M. H. V. (1992) *FASEB J. 6*, 3265−3274.
Betz, S., Fairman, R., O'Neil, K. T., Lear, J., & DeGrado, W. F. (1995) *Phil. Trans. R. Soc. London 348*, 81−88.
Bhat, T. N., Bentley, G. A., Fischmann, T. O., Boulot, G., & Poljak, R. J. (1990) *Nature 347*, 483−485.
Bhat, T. N., Bentley, G. A., Boulot, G., Greene, M. I., Tello, D., Dall'Acqua, W., Souchon, H., Schwarz, F. P., Mariuzza, R. A., & Poljak, R. J. (1994) *Proc. Natl. Acad. Sci. U.S.A. 91*, 1089−1093.
Braden, B. C., & Poljak, R. J. (1995) *FASEB J. 9*, 9−16.
Bundle, D. R., Baumann, H., Brisson, J. R., Gagne, S. M., Zdanov, A., & Cygler, M. (1994) *Biochemistry 33*, 5183−5192.
Crumpton, M. J. (1966) *Biochem. J. 100*, 223−232.
Dyson, H. J., & Wright, P. E. (1995) *FASEB J. 9*, 37−42.
Goding, J. W. (1986) in *Monoclonal Antibodies: Principle and Practice*, Academic Press, London.
Hodges, R. S., Semchuk, P. D., Taneja, A. K., Kay, C. M., Parker, J. M. R., & Mant, C. T. (1988) *Peptide Res. 1*, 19−30.
Jackson, S. E., Moracci, M., ElMasry, N., Johnson, C. M., & Fersht, A. R. (1993) *Biochemistry 32*, 11259−11269.
Jelesarov, I., & Bosshard, H. R. (1994) *Biochemistry 33*, 13321−13328.
Jelesarov, I., Leder, L., & Bosshard, H. R. (1995) *Immunol. Methods* (in press).
Koshland, D. E., Jr., Nemethy, G., & Filmer, D. (1966) *Biochemistry 5*, 365−385.
Leder, L., Wendt, H., Schwab, C., Jelesarov, I., Bornhauser, S., Ackermann, F., & Bosshard, H. R. (1994) *Eur. J. Biochem. 219*, 73−81.
Livingstone, J. R., Spolar, R. S., & Record, M. T., Jr. (1991) *Biochemistry 30*, 4237−4244.
Murphy, K. P., & Freire, E. (1992) *Adv. Protein Chem. 43*, 313−361.
Ngai, P. K., Ackermann, F., Wendt, H., Savoca, R., & Bosshard, H. R. (1993) *J. Immunol. Methods 158*, 267−276.
O'Neil, K. T., & DeGrado, W. F. (1990) *Science 250*, 646−651.
O'Shea, E. K., Rutkowski, R., & Kim, P. S. (1989) *Science 243*, 538−542.
Pace, C. N., Shirley, B. A., & Thomson, J. A. (1989) in *Protein Structure, a Practical Approach* (Creighton, T. E., Ed.) pp 311−330, IRL Press, Oxford, U.K.
Posnett, D. N., & Tam, J. P. (1989) *Methods Enzymol. 178*, 739−746.
Rini, J. M., Schulze-Gahmen, U., & Wilson, I. A. (1992) *Science 255*, 959−965.
Roberts, S., Cheetam, J. C., & Rees, A. R. (1987) *Nature 328*, 731−734.
Schwab, C., & Bosshard, H. R. (1992) *J. Immunol. Methods 147*, 125−134.
Schwarz, F. P., Tello, D., Goldbaum, F. A., Mariuzza, R. A., & Poljak, R. J. (1995) *Eur. J. Biochem. 228*, 388−394.
Shoham, M. (1993) *J. Mol. Biol. 232*, 1169−1175.
Spangler, B. D. (1991) *J. Immunol. 146*, 1591−1595.
Stanfield, R. L., & Wilson, I. A. (1993) *Immunol. Methods 3*, 211−221.
Stanfield, R. L., Fieser, T. M., Lerner, R. A., & Wilson, I. A. (1990) *Science 248*, 712−719.
Sturtevant, J. M. (1977) *Proc. Natl. Acad. Sci. U.S.A. 74*, 2236−2240.
Tam, J. P. (1988) *Proc. Natl. Acad. Sci. U.S.A. 85*, 5409−5413.
Thomas, R. M., Wendt, H., Zampieri, A., & Bosshard, H. R. (1995) *Prog. Colloid Polym. Sci.* (in press).
Thompson, K. S., Vinson, C. R., & Freire, E. (1993) *Biochemistry 32*, 5491−5496.
Tsang, P., Rance, M., Fieser, T. M., Ostresh, J. M., Houghten, R. A., Lerner, R. A., & Wright, P. E. (1992) *Biochemistry 31*, 3862−3871.
Tulip, W. R., Varghese, J. N., Laver, W. G., Webster, R. G., & Colman, P. M. (1992) *J. Mol. Biol. 227*, 122−148.
Wendt, H., Baici, A., & Bosshard, H. R. (1994) *J. Am. Chem. Soc. 116*, 6973−6974.
Wendt, H., Berger, C., Baici, A., Thomas, R. M., & Bosshard, H. R. (1995) *Biochemistry 34*, 4097−4107.
Wien, M. W., Filman, D. J., Stura, E. A., Guillot, S., Delpeyroux, F., Crainic, R., & Hogle, J. M. (1995) *Nature Struct. Biol. 2*, 232−243.
Wilson, I. A., & Stanfield, R. L. (1994) *Curr. Opinion Struct. Biol. 4*, 857−867.
Wiseman, T., Williston, S., Brandts, J. F., & Lin, L.-N. (1989) *Anal. Biochem. 179*, 131−137.
Zhang, L., & Hermans, J. (1993) *Proteins 16*, 384−392.
Zhou, N. E., Kay, C. M., & Hodges, R. S. (1992) *J. Biol. Chem. 267*, 2664−2670.

BI951551I